Bull Volcanol (1995) 57:136–145

ORIGINAL PAPER

J. Camitz · F. Sigmundsson · G. Foulger
C.-H. Jahn · C. Völksen · P. Einarsson

Plate boundary deformation and continuing deflation of the Askja volcano, North Iceland, determined with GPS, 1987–1993

Received June 27, 1994 / Accepted December 23, 1994

Abstract GPS geodetic measurements were conducted around the Askja central volcano located at the divergent plate boundary in north Iceland in 1987, 1990, 1992 and 1993. The accuracy of the 1987 and 1990 measurements is in the range of 10 mm for horizontal components; the accuracy of the 1992 and 1993 measurements is about 4 mm in the horizontal plane. Regional deformation in the Askja region is dominated by extension. Points located outside a 30–45 km wide plate boundary deformation zone indicate a displacement of 2.4 ± 0.5 cm/a in the direction N 99° E $\pm$ 12° of the Eurasian plate relative to the North American plate in the period 1987–1990. Within the plate boundary deformation zone extensional strain accumulates at a rate of ~ 0.8 μstrain/a. Displacement of control points next to Askja (<7 km from the caldera center) in the periods 1990–1993 and 1992–1993 show deflation and contraction towards the caldera. These results are in accordance with the results obtained by other geodetic methods in the area, which indicate that the deflation at Askja occurs in response to a pressure decrease at about 2.8 km depth, located close to the center of the main Askja caldera. A Mogi point source was fixed at this location and the GPS data used to solve for the source strength. A central subsidence of 11 ± 2.5 cm in the period 1990–1993 is indicated, and 5.5 ± 1.5 cm in the period 1992–1993. The maximum tensional strain rate, according to the point source model, occurs at a horizontal distance of 2.5–6 km from the source, at the same location as the main caldera boundary. Discrepancies between the observed displacements and predicted displacements from the Mogi model near the Askja caldera can be attributed to the regional east–west extension that occurs at Askja.

Key words GPS · Askja central volcano · Caldera · Deformation · Plate boundary zone · Magma chamber

Johan Camitz · Freysteinn Sigmundsson (✉)
Nordic Volcanological Institute, University of Iceland, IS 101 Reykjavik, Iceland. Tel.: 354 569 4492. Fax.: 354 562 9767. E-mail: fs@norvol.hi.is

Gillian Foulger
Department of Geology, University of Durham, Durham, UK

Cord-Hinrich Jahn · Christof Völksen
Institut für Erdmessung, Universität Hannover, Hannover, Germany

Pall Einarsson
Science Institute, University of Iceland, Reykjavik, Iceland

Introduction

The Askja volcanic complex is located within the Askja fissure swarm at the divergent plate boundary in north Iceland (Fig. 1). The fissure swarm is 10–15 km wide and more than 100 km long. The volcanic complex is built up by subaerially erupted basaltic lava and subaquatic hyaloclastites and pillow lavas (Sigvaldason 1968). In the early Holocene a caldera was formed (Sigvaldason 1979). The caldera has a diameter of about 8 km and an area of about 50 km^2. The caldera floor has an elevation of about 1100–1200 m, whereas the surrounding margins rise about 200–400 m. One major volcano-tectonic episode is known in the Askja volcanic system during the last few centuries. It occurred in 1874–1876 and included several basaltic fissure eruptions in the fissure swarm and a major plinian eruption of Askja volcano (Sigvaldason 1979; Sigurdsson and Sparks 1978; Brandsdottir 1992). A new caldera was formed during this episode, 4.5 km in diameter and 15 km^2 in area, nested in the south-eastern part of the old caldera. The caldera floor dropped about 230 m and is now occupied by Lake Öskjuvatn. Another, less significant, episode of activity occurred in 1921–1929. It included several small eruptions around the Öskjuvatn caldera with an erupted volume of about 0.03 km^3, and a larger fissure eruption south of the caldera with an estimated lava volume of 0.3 km^3 (Sigvaldason et al. 1992). There are some indications that part of this lava

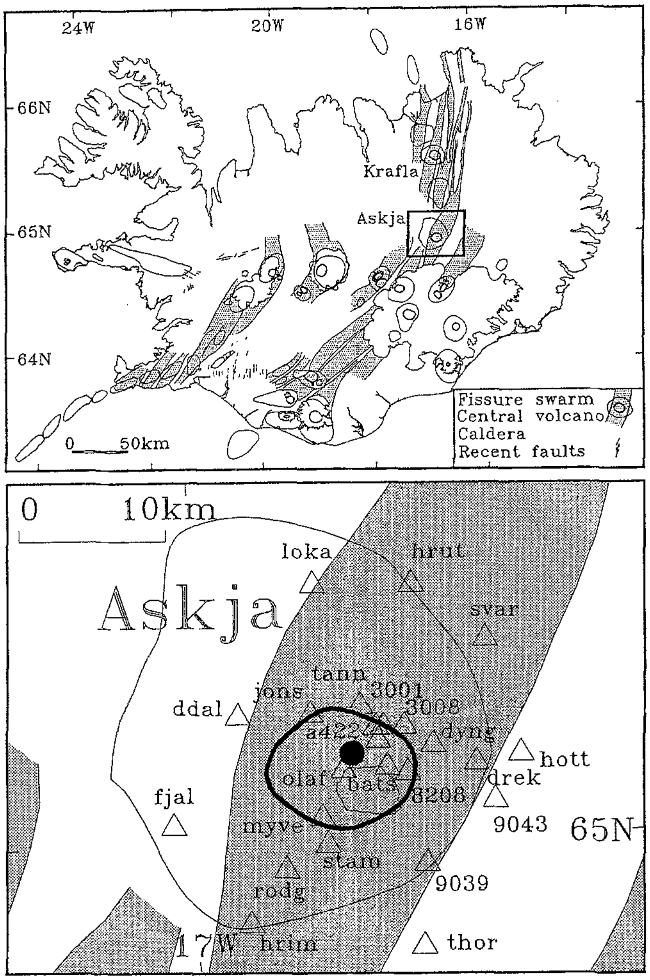

Fig. 1 **a** Map of Iceland showing fissure swarms (shaded), central volcanoes (outlined), calderas (heavy outlines) and recent faults. Glaciers are also outlined. Location of Fig. 1b indicated by the box. After Einarsson and Saemundsson (1987). **b** Map of the Askja area with GPS points of the 1993 survey. Fissure swarms are dotted; heavy outline marks the Askja caldera. Thin outline within the Askja caldera outlines the Lake Öskjuvatn caldera, and thin outline outside the Askja caldera marks the limit of the Askja central volcano. Location of the center of subsidence in Askja according to Rymer and Tryggvason (1993) is shown as a closed circle

south of the caldera was erupted earlier (E. Tryggvason, personal communication 1994). The eruptive fissure is directed ~N30°E, dominated by the regional stress field which has the axis of minimum compressive stress perpendicular to the strike of the fissure swarm. A third episode of activity occurred in 1961–1962 and consisted of an eruption of 0.09 km^3 of basalt and two possible intrusion events (Brandsdottir 1992; Sigvaldason et al. 1992).

Deformation at Askja has been monitored since 1966 using several geodetic methods (Tryggvason 1989a, 1989b; Rymer and Tryggvason 1993). In the period 1966–1972 vertical deformation was measured yearly by precision leveling, and by lake level observations of Lake Öskjuvatn. No measurements were carried out in the period 1973–1981. Leveling has been conducted yearly since 1983, and in 1988 and 1990 nine optical leveling tilt (dry tilt) stations were installed. Electronic distance measurements were made in 1982, 1985, 1986 and 1993. Microgravity monitoring has been performed regularly at the Askja volcano since 1988. Deflation of the volcano occurred at a rate of a few centimeters per year in the period 1966–1967, inflation in 1967–1968 and deflation in 1968–1970. In 1970–1972 rapid inflation occurred at a rate of about 20 cm/a. During the period 1972–1983 a net deflation of 20 cm occurred. Since 1983 deflation at a rate of 4–6 cm/a is indicated by the measurements. Most of the ground deformation in Askja can be explained as a response to pressure changes in a shallow magma chamber. A Mogi point source, located approximately at the center of the main Askja caldera, is adequate to model most of the data (Tryggvason 1989a). In particular, on the basis of tilt measurements in the period 1988–1991, Rymer and Tryggvason (1993) conclude that 80% of the ground deformation in Askja can be explained by a source located at 65° 3.19′ N, 16° 46.10′ W, and at a depth of 2.8 ± 0.3 km (Fig. 1).

Regional GPS surveys were conducted in north Iceland in 1987, 1990 and 1992. The aim was to monitor crustal deformation across the plate boundary in north Iceland. Some points in the southern part of this network are located in the vicinity of Askja, but most of them are too far away from the Askja caldera to be affected by deformation caused by a shallow magma chamber there. Comparison of the 1987 and 1990 data revealed east–west expansion across the plate boundary in north Iceland (Foulger et al. 1992; Heki et al. 1993; Jahn 1992a, 1992b). Widening of up to 5 cm/a across the Krafla fissure swarm, compared with full plate velocities of 1.9 cm/a according to the NUVEL-1 global plate motion model (DeMets et al. 1990), has been attributed to post-rifting stress relaxation after the 1975–1984 Krafla rifting episode when a 80 km long segment of the Krafla fissure swarm widened on average by 4–6 m (Tryggvason 1984; personal communication 1993). In this paper we discuss regional deformation near Askja in the 1987–1990 period, and then present new results based on GPS data collected on an extended network near the Askja volcano in 1992 and 1993 (Table 1). A horizontal displacement solution for the period 1987–1990 is used to study crustal widening across the rift zone in the Askja area. The 1990, 1992 and 1993 coordinate solutions are subsequently used to study local deformation of Askja volcano.

GPS measurements 1987–1993

The regional GPS network established in 1987 in north Iceland consisted of 63 points, centered on the rift zone in north-east Iceland and extending 130 km into the plates. Most of the GPS points in the network were remeasured in 1990, and some new points were added.

Table 1 Stations occupation in GPS surveys in the Askja area, excluding the 1992 regional GPS survey. For the years 1987 and 1990, the table only includes GPS points near Askja, not all the GPS points occupied in north Iceland during these years. Two-digit numbers for station names are identification numbers used in 1987 and 1990. All points are shown in Fig. 1 and/or Fig. 3. *L* is approximate distance of stations from the DYNG station, our reference station

Station name	*L* (km)	1987	1990	1992	1993
Dyng (49)	0	X	X	X	X
42	39.8	X	X		
43	36.8	X	X		
47	60.9	X	X		
51	21.7	X	X		
52	33.7	X	X		
54	52.1	X	X		
55	23.8	X	X		
56	34.7	X	X		
63	24.9	X	X		
64	38.0	X	X		
65	23.1	X	X		
66	40.3	X	X		
67	30.6	X	X		
Fjal (48)	18.7	X			X
Thor (50)	13.8	X	X		X
A404 (70)	3.8		X		X
Hott (72)	6.1		X		X
Loka (73)	13.7		X		X
Stam (74)	9.9		X		X
Hrim (75)	17.4		X		X
3001	3.7			X	X
3008	2.4			X	X
9039	8.1			X	X
9043	5.7			X	X
8208	2.6				X
A422	4.1				X
Ddal	13.5				X
Hrut	11.1				X
Svar	8.1				X
Drek	3.2				X
Tann	5.7				X
Bats	3.5				X
Olaf	6.4				X
Jons	8.7				X
Rodg	13.1				X
Myve	9.1				X

Table 2 Approximate 1σ uncertainty of GPS surveys in north Iceland

	North (mm)	East (mm)	Vertical (mm)
1987	6	9	16
1990	10	11	19
1992	4	4	7
1993	4	4	8

The surveys were a co-operative project between University of Hannover, the University of Durham and several Icelandic institutions. Data analysis was conducted in two independent ways; the results have been described in detail by Heki et al. (1993) and Jahn (1992b). The Hanover group used the GEONAP software (Wübbena 1989) and the Durham group used the BERNESE software (Rothacher et al. 1990) to analyze the data. The two coordinate solutions show satisfactory agreement, documented by Heki et al. (1993). We only summarize here the relevant features of the BERNESE results chosen for our deformation analysis. The additional data presented here, from the 1992 and 1993 surveys, have also been analyzed with this software. Uncertainty is estimated from the session to session scatter (repeatability), defined as the weighted root mean square of the differences between the coordinates from individual sessions and a network solution. In this paper we assume that the session to session scatter is a measure of 1σ uncertainty, summarized in Table 2. More detailed error analysis of the 1987 and 1990 data are presented by Jahn (1992b). The derived error ellipses for the horizontal station coordinates are approximately circles. The main effect of the improved satellite constellation on the 1992 and 1993 surveys, when compared with the earlier surveys, has been to reduce coordinate errors without modifying the shape of the horizontal station coordinate error ellipses significantly. The DYNG station served as a reference station in 1992 and 1993 and was occupied continuously during these surveys; it was also used as a reference station in 1987 and 1990 when the stations next to Askja were measured. The inclusion of a common reference point during all the observation sessions, and the calculation of station coordinates relative to this reference point, ensures that covariance among the station positions in the GPS network is minimal.

1987–1990

Seven TI-4100 GPS receivers were used in these surveys. Most GPS points were measured on two different days. In 1987 the measurement sessions were 3.3 hours long, and in 1990 they were 4.2 hours long. The observation interval was 30 seconds. The final coordinates were derived from ionospheric-free, phase ambiguity fixed solutions from each session, combined into a network solution. The estimated 1σ accuracy, based on the session to session scatter, of the 1987 BERNESE solution is 6, 9 and 16 mm for the north, east and vertical components, respectively (Heki et al. 1993). Most of the stations measured in 1987 were remeasured in 1990, and the data were analyzed in the same way as before. Severe ionospheric conditions during this survey made the resolution of the L1 and L2 ambiguities difficult, and ambiguity resolution was abandoned in the BERNESE solution. The estimated accuracy of the 1990 BERNESE solution is 10, 11 and 19 mm for the north, east and vertical components, respectively (Heki et al. 1993). Broadcast orbits were used, although some baseline lengths exceeded 100 km. A comparison of coordinate solutions based on broadcast and IGS (International GPS Service for Geodynamics) precise orbits for a similar scale regional GPS network in south Iceland measured in 1992 (Sigmundsson et al. 1995) suggests that the coordinate accuracy of the 1987 and 1990 surveys could be improved by only a few millimeters by the use of precise orbits. This has not been carried out.

1992–1993

The regional GPS network in north Iceland was remeasured again in 1992, but the results from this survey are not reported here. The first measurements to densify the GPS network at Askja volcano were conducted during a separate survey in 1992. Four new GPS points, and the DYNG reference station, were measured 26–29 August, 1992, within 11 km of the center of Askja caldera. Unfavorable weather conditions limited the measurement period to only three days. A more extensive survey was conducted at Askja volcano on 5–20 August, 1993. During this time 24 GPS points were measured in and near Askja caldera. Twelve of the points had been measured at least once before, and 12 new points were installed (Table 1). The points measured in the 1993 GPS survey are within 15 km of the center of Askja caldera (Fig. 1). The 1992 and 1993 GPS surveys were conducted and analyzed in the same manner. Three TRIMBLE 4000 SST GPS receivers were operated almost continuously during the surveys. The observation interval was 15 seconds. Each day was devided into three eight hour long sessions to obtain independent measurements. Tripods were, however, not reset between sessions. The reference station, DYNG, was held fixed and occupied during the entire survey period. Most other control points were occupied for three adjacent measurement sessions.

The data were analyzed using Version 3.3 of the BERNESE GPS software using broadcast orbits. Broadcast orbits were chosen rather than precise IGS orbits because of the short baselines occupied and to provide coordinates directly comparable with the 1987 and 1990 coordinates in the WGS-84 coordinate system. The original L1 and L2 phase carrier signals were combined to obtain the L3 and L5 linear combinations. The L3 linear combination is almost free of ionospheric effects and the L5 (wide lane) combination has a much longer wavelength than L1, L2 or L3. The Saastamoinen troposphere model, assuming standard meteorological conditions, was used to model atmospheric effects. Carrier phase cycle slips were mostly fixed automatically using the program MAUPRP. Few remaining cycle slips were detected manually using the program XSLIP (UNAVCO 1991) and subsequently fixed. With the data free of cycle slips, an L3 solution was calculated for each measurement session, with unresolved phase ambiguities using the parameter estimation program GPSEST. The L5 ambiguities (the difference between the L1 and L2 ambiguities) were then resolved holding the coordinates obtained in the previous L3 solution fixed. The L1 and L2 ambiguities were then resolved using the L5 ambiguities. The final solution for each session is an ionospheric-free solution with fixed phase ambiguities. The ambiguity resolution was successful for the 1992 data (92% of the ambiguities could be resolved to integers) and for the 1993 data (94% of the ambiguities could be resolved to integers). The ambiguity resolution caused about 50% reduction in the session to session scatter for the horizontal components, but no improvement occurred for the vertical components. To produce final coordinates for each survey, we used the weighted average of station coordinates from all sessions.

In 1992 and 1993 each station was occupied for at least three sessions, providing at least three coordinate values, and we calculated coordinate residuals from the weighted average value for each station (Fig. 2). The average rms value of the session to session scatter, σ_{scatter}, is about 2 mm in the north, east and length direction and 7 mm in the height direction. The session to session scatter does not take into account antenna setup errors, σ_{setup}, which are correlated during different sessions, as we used only one antenna setup for each point. We estimate these to be about 2 mm at all stations. The estimated total one standard deviation uncertainty in a point location relative to the base station is

$$\sigma = \sqrt{\sigma^2_{\text{scatter}} + 2\,\sigma^2_{\text{setup}}} \tag{1}$$

where σ is the estimated one standard deviation uncertainty. The $2\,\sigma^2_{\text{setup}}$ accounts for antenna setup errors at both ends of the baselines. This formula applies to all the coordinate components: north, east, vertical and length of vectors from the reference site to the other sites. For $\sigma_{\text{setup}} = 2$ mm, we estimate the uncertainty to be about 4 mm in the north, east and length components and 8 mm in height for the 1993 survey. For the 1992 survey we estimate a 1σ uncertainty of 4 mm in the horizontal components and 7 mm in the vertical. We ignore the correlation between the east and north coordinate components, as the observed session to session scatter is the same for these components. We have also not considered the formal solution coordinate uncertainties provided by the BERNESE software. These are an order of magnitude smaller than the session of session scatter, but are similar for most of the stations. The improved accuracy of the 1992 and 1993 data when compared with the 1987 and 1990 data is caused by improved satellite constellation, shorter baselines and by longer observation sessions in 1992 and 1993 than before.

Method of interpretation

The coverage of GPS points near Askja volcano was very limited before the 1993 survey, and the leveling, optical tilt and lake level observations still provide better information on the source of deformation within the caldera. From these measurements a pressure source near the center of the main Askja caldera has been identified; the GPS data are also consistent with a

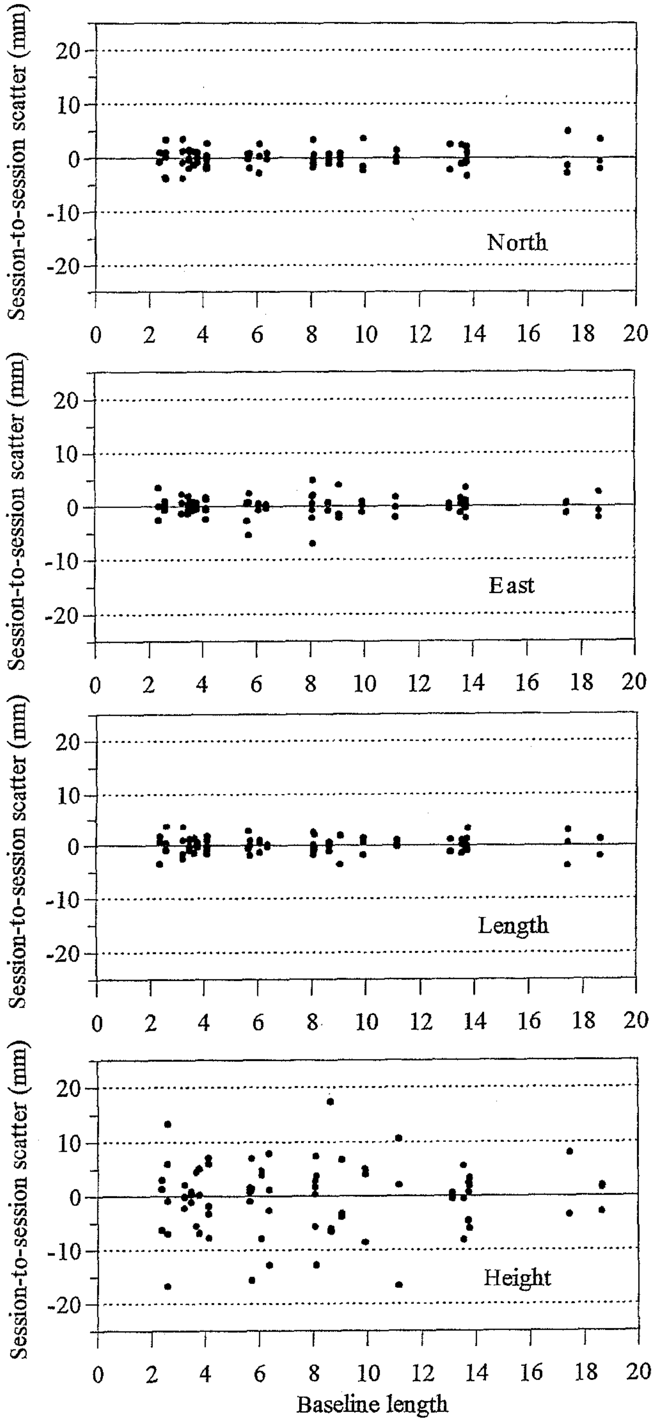

Fig. 2 Session to session scatter of the 1993 final results for the north, east, line length and height versus line length. Coordinate residuals from the weighted average solution are shown

source in this location. To limit a wide range of models consistent with the GPS data, because of the limited number of remeasured GPS points, we used the previously determined location of the pressure source as a constraint in our modeling. We fix a pressure source at 65° 3.19′ N, 16° 46.10′ W, and at 2.8 km depth, the values reported by Rymer and Tryggvason (1993), and solve only for the source strength using the GPS data. The Mogi model assumes a small sphere with varying pressure, a point source, in an elastic half-space. The horizontal, Δd, and the vertical, Δh, displacements on the surface are (Mogi 1958)

$$\Delta d = C\frac{d}{(f^2+d^2)^{3/2}} \tag{2}$$

$$\Delta h = C\frac{f}{(f^2+d^2)^{3/2}} \tag{3}$$

where f is the depth to the point source, C is the strength of the source and d is the horizontal (radial) distance at the surface from the point source. The strength parameter equals $3a^3\Delta P/4\mu$ where a is the radius of the spherical source, ΔP is the change in the pressure at the source and μ is the rigidity of the elastic half-space. The strength parameter, C, is related to the vertical displacement at the surface directly above the point source, Δh_0, such that $C=\Delta h_0 f^2$. The Mogi model is valid when the ratio $(a/f)^5 \ll 1$ (McTigue 1987). As $(a/f)^5$ is still only 0.03 when $f=2a$, the Mogi equations apply fairly well for finite sized magma chambers, as well as for point sources. We use a least-squares criterion to find the best-fitting Mogi source strength, using both horizontal and vertical displacements relative to our base station. We vary the value of C to minimize the χ^2 merit function

$$\chi^2 = \sum_{i=1}^{N}\left(\frac{\delta \boldsymbol{r}_i^{\text{obs}}(\boldsymbol{r}_i) - \delta \boldsymbol{r}_i^{\text{pre}}(\boldsymbol{r}_i; C)}{\sigma_i}\right)^2 \tag{4}$$

where $\boldsymbol{r}_i$ is the horizontal location (latitude and longitude) of control point i, $\delta\boldsymbol{r}_i^{\text{obs}}(\boldsymbol{r}_i)$ is the observed three-dimensional relative displacement vector at location $\boldsymbol{r}_i$, and $\delta\boldsymbol{r}_i^{\text{pre}}(\boldsymbol{r}_i; C)$ is the predicted relative displacement. N is the number of relative displacement vectors, and σ_i is the uncertainty in $\delta\boldsymbol{r}_i^{\text{obs}}(\boldsymbol{r}_i)$. The minimum value for χ^2 occurs at the best-fitting value for C. If the model is consistent with the data, and measurement errors are normally distributed, χ^2 is distributed as a chi-square distribution with $3N-M$ degrees of freedom. $3N$ is the number of vector components that we model and M is the number of adjustable model parameters, one in this instance. A variation in C from the best-fitting value, which will cause an increase in χ^2 from χ^2_{min} by one, is an estimate of the 1σ uncertainty in the value of C (Bevington 1969:243). As the covariance among station positions during individual surveys is small, because of the inclusion of a common reference point during all observation sessions, the covariance of station displacements is also small and ignored here.

Deformation

1987–1990

Comparison of the 1987 and 1990 coordinates reveals east–west expansion across the plate boundary in north

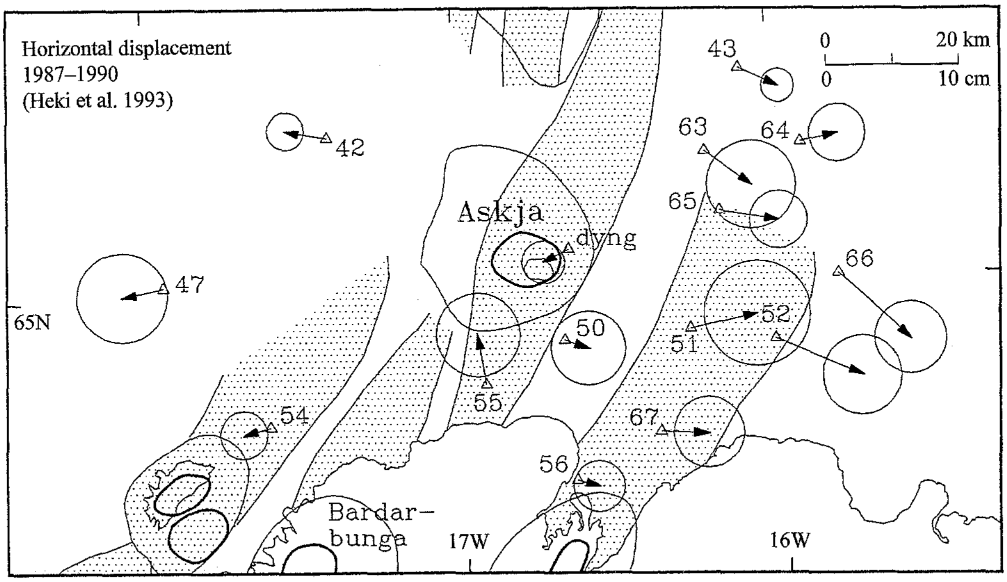

Fig. 3 Horizontal displacements in the period 1987–1990. Modified from Heki et al. (1993). Circles are approximate 1 σ uncertainties, based on formal solution errors of the Heki et al. (1993) solution scaled to reflect the session to session scatter. The radius of the circles represents the average of the north–south and east–west components of errors. In most cases both components are similar

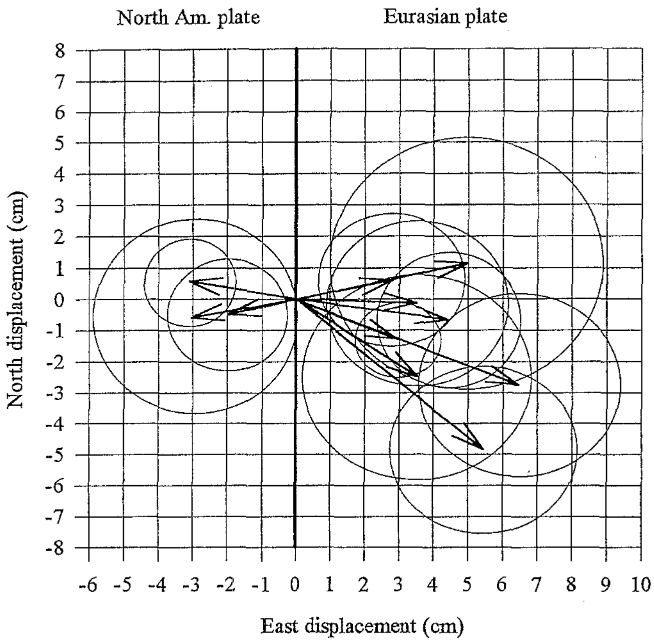

Fig. 4 Horizontal displacement vectors for the period 1987–1990, excluding points within the plate boundary deformation zone. The vectors are plotted with a common origin. All vectors pointing to the east are from the Eurasian plate, and vectors pointing west are from the North American plate. Internal deformation within the plates is insignificant as the approximate 1 σ error circles overlap. By averaging the displacements we deduce a spreading rate of 2.4 ± 0.5 cm/a in the direction N 99° E ± 12° of the Eurasian plate relative to the North American plate

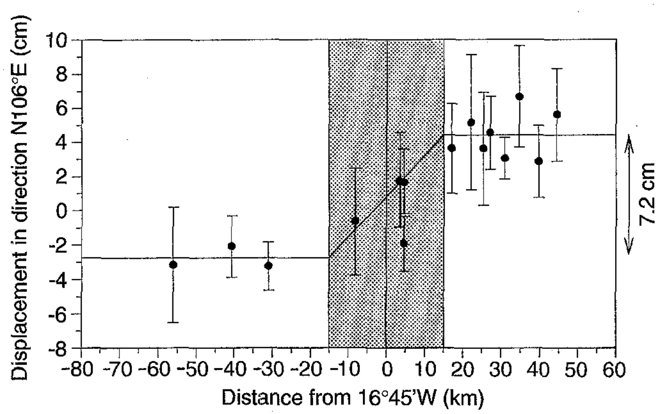

Fig. 5 Displacements, with 1 σ error bars, in direction N 106° E, the NUVEL-1 spreading direction, for the period 1987–1990. Displacements are plotted versus distance from 16° 45′ W (a north–south line crossing Askja). The observed full spreading rate is 2.4 cm/a. We infer that the plate boundary deformation zone is approximately 30 km wide (shaded). If a constant strain rate is assumed within this zone, displacements increase linearly with distance within it. The point within the plate boundary deformation zone not falling on the same line as the others is affected by the shallow magma chamber at Askja

Iceland (Fig. 3). We studied a subset of 15 points occupied during these surveys: three are located west of the plate boundary (on the North American plate), eight to the east (on the Eurasian plate) and four points are considered to be located within a plate boundary deformation zone. When displacement vectors are plotted with a common origin (Fig. 4), it is evident that the approximate 1 σ error circles overlap in the areas east and west of the plate boundary, consistent with little internal deformation within the plates. We average the vectors in these areas to estimate the divergence of the North American plate relative to the Eurasian plate. The divergence is 2.4 ± 0.5 cm/a in direction N 99° ± 12° E. The NUVEL-1 global plate motion model (DeMets et al. 1990) predicts a divergence of 1.90 cm/a in the direction N 106° E, a value which is within our uncertainty limits. Based on the GEONAP displacement solution for the period 1987–1990, Jahn (1992a, 1992b) estimates the divergence to be 2.2 ± 0.3 cm/a in agreement with our findings. A plot of displacement versus east–west distance from Askja (Fig. 5) shows that the full spreading rate is obtained at an east–west distance of about 15–30 km. We infer that the plate boundary deformation zone is about 30–45 km wide at the present time. The DYNG station close to Askja caldera indicates contraction towards the caldera, but only at the 1σ uncertainty level, caused by deflation in the 1987–1990 period. Within the plate boundary deformation zone not affected by deflation of Askja volcano, displacements increase from zero to the full spreading rate to accommodate the regional extension. As there are only four GPS points within the plate boundary deformation zone, there is limited information on the shape of the displacement profile within the zone. To a first approximation we assume a constant strain rate within the plate boundary deformation zone; accordingly, displacements will increase linearly with distance from the center of the zone. For a zone 30 km wide with plate movements of 2.4 cm/a, the strain rate within the zone is 0.8 μstrain/a.

1990–1993

We initially calculated the displacements of GPS points relative to the DYNG station, our base station. We then fitted a Mogi source model to these relative displacements. For each vector component, the 1σ displacement uncertainty is estimated as $(\sigma^2_{1990}+\sigma^2_{1993})^{1/2}$, where σ_{1990} and σ_{1993} are the uncertainties in the 1990 and the 1993 locations. The 1σ displacement uncertainties estimated in this way are 12 mm in the horizontal and 21 mm in the vertical directions. We used five displacement vectors relative to the base station for the 1990–1993 displacement analysis. The minimum χ^2 value was 13.6 for $C=-0.86\pm0.2\times10^6\ \mathrm{m}^3$ and the corresponding maximum subsidence, Δh_0, was 11 ± 2.5 cm for the three year period (1σ uncertainties). A statistical chi-square test shows the GPS data are consistent with the model. The best-fitting model predicts a displacement for the base station of 2.01 cm in direction 266°. This displacement is added to all the relative displacements. The estimated horizontal displacements in the period 1990–1993 then show contraction approximately towards the center of the caldera, for two points located close to the volcano (Fig. 6). More distant points show displacements more influenced by the regional extension across the plate boundary. The best-fit Mogi curves show a reasonable agreement in the horizontal component, but a much poorer fit for the vertical component.

1992–1993

Five points are common to the 1992 and 1993 surveys. The 1σ uncertainties of the displacements for the period 1992–1993 are estimated 6 mm for the horizontal component and 11 mm for the vertical. Using the same approach as for the 1990–1993 displacements, we find $\chi^2_{\min}=10.0$ for C equal to $-0.43\pm0.12\times10^6\ \mathrm{m}^3$. The corresponding maximum subsidence, Δh_0, is

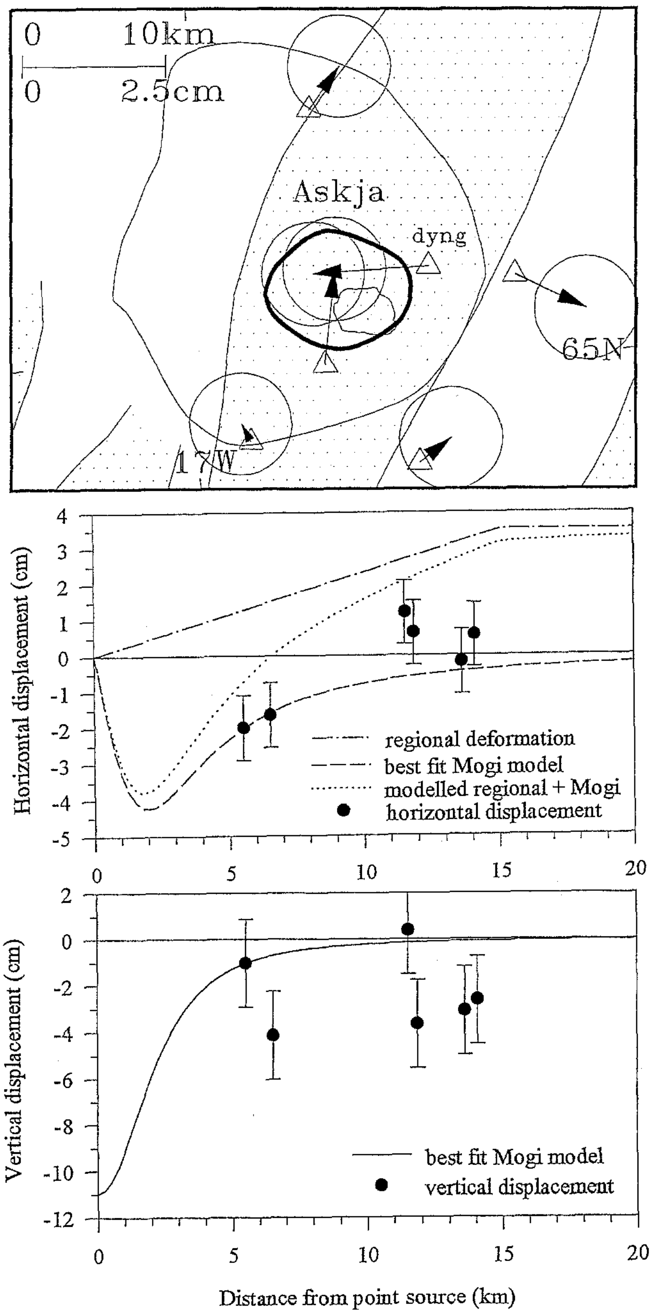

Fig. 6 **a** Horizontal displacements in the period 1990–1993. A displacement of 2.01 cm in direction 266° is assumed for the reference station DYNG, in accordance with a best-fitting Mogi model as explained in the text. Circles represent approximate 1σ uncertainties based on the average session to session scatter. **b** Measured horizontal displacements 1990–1993 versus distance from point source. Best-fitting Mogi curve, estimated regional deformation based on the 1987–1990 data, and combined Mogi and regional deformation in the spreading direction. **c** Vertical displacements in the period 1990–1993 versus distance from the point source

5.5 ± 1.5 cm. The best-fitting vector for the DYNG station is 1.01 cm in direction 266°. The general trend of the deformation is a deflation with increasing vertical displacement towards the caldera. Three points close to the caldera show contraction towards the caldera center

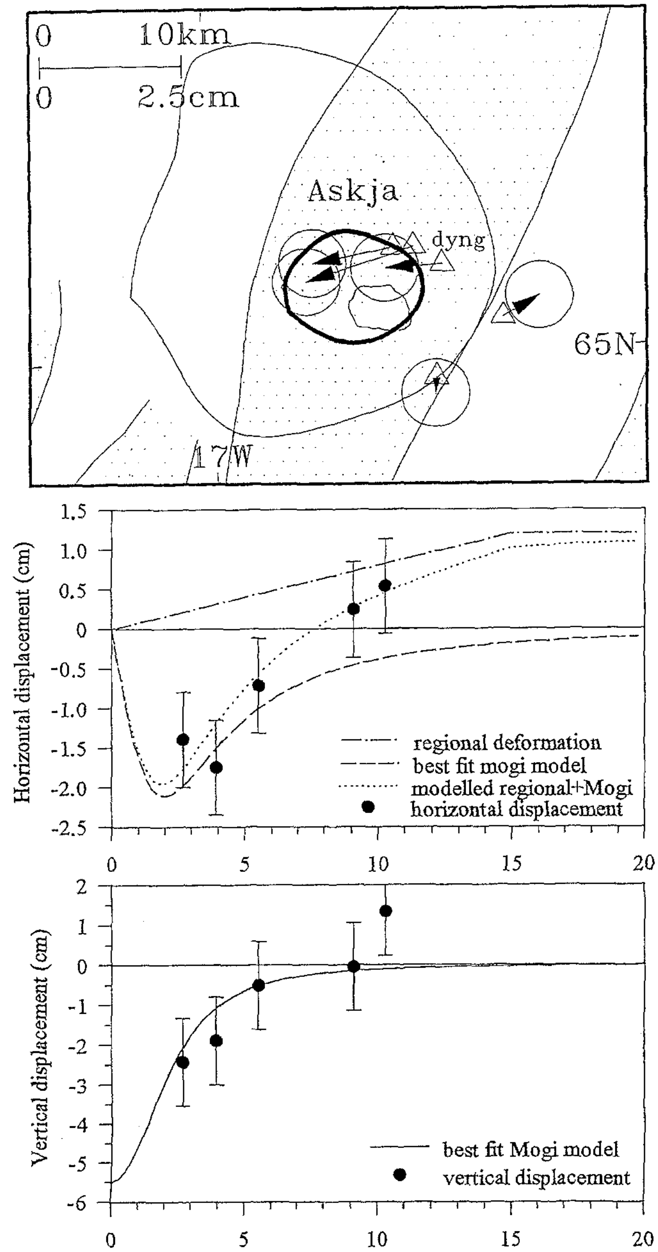

Fig. 7 **a** Horizontal displacements in the period 1992–1993. A displacement of 1.01 cm in direction 266° is assumed for the reference station DYNG, in accordance with a best-fitting Mogi model. Circles represent approximate 1 σ uncertainties based on the average session to session scatter. **b** Measured horizontal displacements 1992–1993 versus distance from point source. Best-fitting Mogi curve, estimated regional deformation based on the 1987–1990 data, and combined Mogi and regional deformation in the spreading direction. Notice a different scale than in Fig. 6. **c** Vertical displacements 1992–1993 versus distance from point source

(Fig. 7), but two more distant points show displacements away from the plate boundary due to regional extension. The best-fit Mogi curves show a good fit for both the horizontal and the vertical components.

Discussion

These deformation data are consistent with two deformation processes acting in the vicinity of Askja volcano: extension across the plate boundary and radially symmetrical deflation caused by pressure decrease at a shallow depth near the center of the caldera. The 1987–1990 horizontal displacements of the few control points within the plate boundary deformation zone are consistent with the linear increase in displacement with distance from the center of the zone (Fig. 5). The extensional strain rate, $\dot{\varepsilon}_{\text{ext}}$, within the zone is then constant

$$\dot{\varepsilon}_{\text{ext}} = \frac{\dot{L}}{L} \tag{5}$$

where L is the width of the plate boundary deformation zone and $\dot{L}$ is the rate of extension across the zone. For $L = 30$ km and $\dot{L} = 2.4$ cm/a we find $\dot{\varepsilon}_{\text{ext}} = 0.8$ μstrain/a in the spreading direction. We have not used the distance to the center of the Askja fissure swarm (which strikes about N20°E) in our presentation, rather the east–west distance to a north–south line going through the Askja caldera. The reason for this is that the fissure swarms in north Iceland are arranged in an *en echelon* pattern, and we expect the plate boundary deformation zone to have a more north–south orientation than the Askja fissure swarm. The NUVEL-1 model predicts a spreading rate of 1.90 cm/a in direction N106°E at Askja. Our results imply extension of 2.4±0.5 cm/a in direction N99°±12°E, compatible with the NUVEL-1 model.

The current width of the plate boundary deformation zone at Askja, 30–45 km, is about twice the width of the Askja fissure swarm. It is much less than the current width of the deformation zone at the Krafla fissure swarm in north Iceland (Heki et al. 1993). Crustal velocities measured there exceed the NUVEL-1 velocities out to a distance of more than 100 km from the plate boundary, attributed to post-rifting stress relaxation after the 1975–1985 Krafla rifting episode (Björnsson 1985; Foulger et al. 1992; Heki et al. 1993). The displacements observed in the Askja area are not caused by rifting at Krafla, however. The displacements predicted by Heki et al. (1993) are very small in the Askja area, and they are mainly directed northwards. We attribute the difference in the velocity fields at Askja and Krafla to differences in time since the last rifting episode in the two areas. The velocity field next to the divergent plate boundaries is expected to be highly time dependent; high velocities are expected after a rifting episode and low velocities are expected before a rifting episode (Heki et al. 1993). At Askja we could be at an intermediate stage between major rifting episodes, the last one occurring in 1874–1876. At intermediate times between rifting events, full plate velocities might be expected at smaller distances from the plate boundary than at other times.

The deflation of Askja results in contraction towards the caldera, whereas the regional deformation is extensional. We model the two deformation processes as if they were independent of each other. Points located approximately along the central axis of the plate boundary should only be affected by local deformation. The total horizontal displacement field, on a profile crossing Askja in the spreading direction, is found by adding the predicted regional displacements to the Mogi model displacements. Points at a larger distance from the point source approach the resulting curve very well for the 1992–1993 displacements (Fig. 7b), but less well for the 1990–1993 displacements (Fig. 6b). The more distant points in the 1990–1993 comparison are not oriented in the spreading direction N106°E from the point source, and the displacements of these points are thus expected to be less. According to these models, horizontal displacements on a line from the point source in the spreading direction are directed outward from Askja at a distance of >6.5 km for the 1990–1993 data, and >7.5 km for the 1992–1993 data. The exact location of the cross-over distance is sensitive to the deflation rate. This description of the interplay between local and regional deformation applies between rifting events. During rifting events this interplay will be modified when magma is injected to form dikes, causing compression at the flanks of the rift zone.

The radial strain rate, the derivative of the horizontal radial displacement rate, due to pressure changes in a shallow magma chamber regarded as a point source is

$$\dot{\varepsilon}_{\mathrm{mogi}} = \frac{C(f^2 - 2d^2)}{(f^2 + d^2)^{5/2}} \tag{6}$$

On a profile perpendicular to the spreading direction across Askja, this is the only expected strain. On a profile parallel to the spreading direction across Askja, the regional strain rate adds to the expected strain rate

$$\dot{\varepsilon}_{\mathrm{tot}} = \dot{\varepsilon}_{\mathrm{mogi}} + \dot{\varepsilon}_{\mathrm{ext}} \tag{7}$$

A plot of the radial strain rate predicted from the best-fit Mogi model for the period 1992–1993, and the regional strain rate perpendicular to the rift zone obtained from the 1987–1990 measurements, shows that the regional strain dominates at a distance of ~10 km from the shallow magma chamber (Fig. 8). High extensional strain occurs in the interval 2.5–6 km from the magma chamber with a maximum at a distance of approximately 3.5 km. This is the approximate distance to the caldera boundary from the point source. Askja has been regarded as a typical caldera collapse structure (Saemundsson 1982; Gudmundsson 1988; Sigvaldason et al. 1992), but based on gravity data Brown et al. (1991) conclude that downfaulting of a large central block has not occurred at Askja. Instead the margins may have partly grown by fissure eruptions, an idea first proposed by Sigurdsson and Sparks (1978). Both the hypotheses demand a maximum in the horizontal tensional stress at the caldera boundary, in a similar location to that in which we observe the maximum extensional strain. The source of the current deflation appears to be in the same location as the source that caused the formation of the main caldera of Askja.

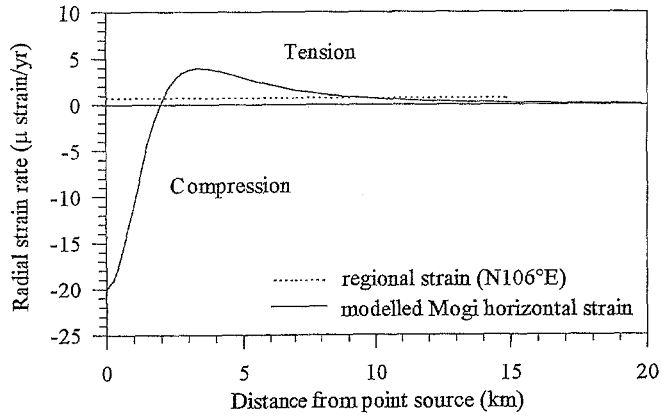

Fig. 8 1992–1993 strain rate according to the best-fit Mogi model, and extensional strain rate across the plate boundary according to the 1987–1990 data (0.8 μstrain/a)

The deflation at Askja is caused by a pressure decrease at shallow depth, but the cause of the pressure decrease is still speculative. Tryggvason (1989a) suggested that the observed inflations and deflations at Askja reflect oscillations of the intensity of convective currents within the Icelandic mantle plume, requiring pressure oscillations in the mantle plume to be transmitted to a shallow magma chamber at Askja. Another explanation may be provided by Einarsson's (1987a, 1987b, 1991) idea that activity at one volcanic system influences the activity of neighboring systems. He suggested that the inflation of the Krafla volcano before and during the Krafla rifting events of 1975–1984 led to a pressure drop in the mantle, which led to the deflation of the crustal magma chambers of neighboring volcanoes. The model was suggested to explain the apparent deflation of the Bardarbunga volcano (shown in Fig. 3), 110 km south of Krafla, but may equally well be applied to Askja, which is located between Krafla and Bardarbunga. Other explanations should also be considered for pressure changes at shallow depth at Askja, explanations that do not require magma to leave a shallow magma chamber. These include the effects of crystallization and cooling of the magma and host rock, which will cause volume contraction and pressure decrease. Also, tensional stress concentration around a shallow magma chamber at Askja due to regional extension across the plate boundary could cause the deflation of Askja volcano. Magma chambers of volcanoes on extensional plate boundaries are continuously being pulled apart to some degree, so long-term continuous subsidence might be the natural state of such volcanoes, even if no magma leaves their magma chambers.

Conclusions

East–west expansion across the Askja fissure swarm in the period 1987–1990 is estimated to be 2.4 ± 0.5 cm/a in the direction N $99° \pm 12°$ E, and the plate boundary deformation zone in the Askja area is currently 30–45 km wide. Point source modeling applies well to horizontal displacements near Askja in the period 1990–1993, and to horizontal and vertical displacements in the 1992–1993 period. The maximum inferred subsidence in the three year period 1990–1993 is 11 ± 2.5 cm, and 5.5 ± 1.5 cm in the period 1992–1993. The variation in deflation rate between the two periods is insignificant, within the 1σ uncertainties. According to previous geodetic work in the area, continuous deflation of Askja has been in progress at least since 1983. A maximum in extensional strain accumulation, according to the best-fit Mogi model, occurs at a distance of 2.5–6 km from the point source, in a similar location to the main caldera boundary. Horizontal displacements of points more than 8 km from the caldera center are clearly influenced by the regional stress field, and currently the regional plate boundary strain field dominates the local magma chamber strain field at a distance of about 10 km or more from Askja.

Acknowledgements We thank Paul Delaney, E. Endo and an anonymous reviewer for thoughtful and comprehensive reviews of the manuscript.

References

Bevington PR (1969) Data Reduction and Error Analysis. McGraw-Hill, New York

Björnsson A (1985) Dynamics of crustal rifting in NE Iceland. J Geophys Res 90:10151–10162

Brandsdottir B (1992) Historical accounts of earthquakes associated with eruptive activity in the Askja volcanic system. Jökull 42:1–12

Brown GC, Everet SP, Rymer H, McGarvie DW (1991) New light on caldera evolution – Askja, Iceland. Geology 19:352–355

DeMets C, Gordon RG, Argus DF, Stein S (1990) Current plate motions. Geophys J Int 101:425–478

Einarsson P (1987a) The anomalous mantle beneath Iceland and possible pressure connection between volcanoes [abstr]. Symposium on How Volcanoes Work, Hilo, 19–25 January 1987

Einarsson P (1987b) Compilation of earthquake fault plane solutions in the North Atlantic and Arctic Oceans. In: Kasahara K (ed) Recent Plate Movements and Deformation. Am Geophys Union Geodyn Ser 20:47–62

Einarsson P (1991) Earthquakes and present-day tectonism in Iceland. Tectonophysics 189:261–279

Einarsson P, Saemundsson K (1987) Earthquake epicenters 1982–1985 and volcanic systems in Iceland. In: Sigfússon Th (ed) Í hlutarins eðli: Festschrift for Thorbjörn Sigurgeirsson. Menningarsjóður, Reykjavik (map)

Foulger GR, Jahn C-H, Seeber G, Einarsson P, Julian BR, Heki K (1992) Post-rifting stress relaxation at the divergent plate boundary in Northeast Iceland. Nature 358:488–490

Gudmundsson A (1988) Formation of collapse calderas. Geology 16:808–810

Heki K, Foulger GR, Julian BR, Jahn C-H (1993) Plate dynamics near divergent boundaries: geophysical implications of post-rifting crustal deformation in NE Iceland. J Geophys Res 98:14279–14297

Jahn C-H (1992a) Recent crustal movements in the neovolcanic zone of Iceland between 1987 and 1990 using GPS. Paper presented at the 6th International FIG-Symposium on Deformation Measurements, 24–28 February 1992, Hannover

Jahn C-H (1992b) Untersuchungen über den Einsatz des Global Positioning Systems (GPS) zum Nachweis rezenter Erdkrustenbewegungen im Spaltengebiet Nordost-Islands. PhD Thesis, Institut für Erdmessung, Universität Hannover

McTigue DF (1987) Elastic stress and deformation near a finite spherical magma body: resolution of the point source paradox. J Geophys Res 92:12931–12940

Mogi K (1958) Relations between the eruptions of various volcanoes and the deformations of the ground surfaces around them. Bull Earthquake Res Inst Univ Tokyo 36:99–134

Rothacher M, Beutler G, Gurtner W, Schildknecht T, Wild U (1990) Documentation for Bernese GPS Software Version 3.2. University of Bern, Bern

Rymer H, Tryggvason E (1993) Gravity and elevation changes at Askja, Iceland. Bull Volcanol 55:362–371

Saemundsson K (1982) Öskjur a virkum eldfjallasvaedum a Islandi (Calderas within the active volcanic zones of Iceland). In: Thorarinsdottir H, Oskarsson OH, Steinthorsson S, Einarsson Th (eds) Eldur er i nordri (Fire in the north). Sögufelag, Reykjavik, pp 221–239

Sigmundsson F, Einarsson P, Bilham R, Sturkell E (1995) Rift-transform kinematics in South Iceland: deformation from Global Positioning System measurements, 1986–1992. J Geophys Res, in press

Sigurdsson H, Sparks RSJ (1978) Rifting episode in northern Iceland in 1874–1875 and the eruptions of Askja and Sveinagja. Bull Volcanol 41:149–167

Sigvaldason GE (1968) Structure and products of subaquatic volcanoes in Iceland. Contr Mineral Petrol 18:1–16

Sigvaldason GE (1979) Rifting, magmatic activity and interaction between acid and basic liquids. The 1875 Askja eruption in Iceland. Nord Volc Inst Rep 7903, 54 pp

Sigvaldason GE, Annertz K, Nilsson M (1992) Effect of glacier loading/deloading on volcanism: postglacial volcanic production rate of the Dyngjufjöll area, central Iceland. Bull Volcanol 54:385–392

Tryggvason E (1984) Widening of the Krafla fissure swarm during the 1975–1981 volcano-tectonic episode. Bull Volcanol 47:47–69

Tryggvason E (1989a) Ground deformation in Askja, Iceland: its source and possible relation to flow of the mantle plume. J Volcanol Geotherm Res 39:61–71

Tryggvason E (1989b) Measurement of ground deformation in Askja 1966 to 1989. Nord Volcanol Inst Rep 8904

UNAVCO (1991) Documentation for Bernese V3.3 Processing with UNAVCO C-Shells. University Navstar Consortium, Boulder

Wübbena G (1989) The GPS adjustment software package – GEONAP – concepts and models. Paper presented at the Fifth International Geodetic Symposium on Satellite Positioning, Defense Mapping Agency and National Geodetic Survey, Las Cruses, New Mexico

Editorial responsibility: W. Hildreth